Structure−Property Relationships for Poly(pyrrolone-imide) Gas Separation Membranes

Ryan L. Burns[‡] and William J. Koros*[,†]

School of Chemical Engineering, Georgia Institute of Technology, Atlanta, Georgia 30332, and The University of Texas at Austin, Austin, Texas 78712

Received December 6, 2002; Revised Manuscript Received February 4, 2003

ABSTRACT: Previous studies have examined polypyrrolone and polyimide membranes for gas separations. For the first time this study examines poly(pyrrolone-imide) copolymers for the O_2/N_2, CO_2/CH_4, and C_3H_6/C_3H_8 separation. Combining these two classes of polymers is designed to provide rigidity and desirable mechanical properties in addition to high-quality gas transport properties. Specifically, the copolymer 6FDA-TAB/DAM was studied while systematically varying the TAB/DAM ratio in order to quantitatively alter the structure of the polymer matrix. Most copolymers studied exhibited results near or above the "upper bound" for O_2/N_2, CO_2/CH_4, and C_3H_6/C_3H_8 separations. Surprisingly, a maximum in C_3H_6/C_3H_8 selectivity was found as a function of the TAB/DAM ratio, and this does not follow the trend expected based on previous literature data. A similar trend has also been observed in carbon molecular sieve materials with varying material structure. This demonstrates that certain materials may show excellent size selective properties for one application (O_2/N_2 for example) and exhibit undesirable separation properties for a different application (C_3H_6/C_3H_8 in this case).

1. Introduction

Efforts to improve polymeric gas separation membranes beyond Robeson's 1991 upper bound tradeoff have achieved a limited amount of success for many applications.[1] However, one area of success has come with polypyrrolone materials, and specific polypyrrolone materials have been shown to possess results above the upper bound for both O_2/N_2 and CO_2/CH_4 separations.[2] These ultrarigid polymers have been called polymeric molecular sieves because they have exhibited entropic selectivity capabilities, similar to carbon molecular sieves and zeolites. In this work, the strategy of achieving a polymeric molecular sieve will be extended using a new class of poly(pyrrolone-imide) copolymers. This strategy is also extended to include the application of olefin/paraffin separations, which has been proposed previously.[3] To our knowledge, there are currently no membranes for olefin/paraffin separations in commercial use, and this market could potentially be reached with a significant breakthrough in polymeric membrane materials.[4]

While many studies have examined different polymeric structures for membrane gas separations, only a limited number of studies have systematically varied the molar ratio of a copolymer in order to quantitatively understand the effect that structure has on the transport characteristics of multiple gas penetrants. This article reports the gas transport properties for a series of semiladder poly(pyrrolone-imide) copolymers for a variety of gas molecules including O_2/N_2, CO_2/CH_4, and C_3H_6/C_3H_8.

2. Background and Theory

Gas transport in polymers and molecular sieve materials can be well described with the solution-diffusion mechanism. The permeability coefficient of a particular penetrant gas can be expressed as the product of the average diffusion coefficient, D_A, and a thermodynamic term in the solubility coefficient, S_A.[5]

$$P_A = D_A S_A \tag{1}$$

The ideal selectivity ($\alpha_{A/B}$) of a membrane material is the ratio of the permeability coefficients of a penetrant pair for the case where the downstream pressure is negligible relative to the upstream feed pressure. Upon substitution of eq 1, the ideal selectivity can also be expressed as a product of the diffusivity selectivity and solubility selectivity of the particular gas pair:

$$\alpha_{A/B} = \frac{P_A}{P_B} = \frac{D_A}{D_B}\frac{S_A}{S_B} \tag{2}$$

The variation of gas permeability with pressure in glassy polymers is often represented by the dual mode and partial immobilization model.[6−8] The model accounts for the differences in gas transport properties in both the idealized Henry's law and Langmuir domains of a glassy polymer. The pressure dependence of solubility for a single component is given by

$$S = \frac{c}{p} = k_D + \frac{C'_H b}{1 + bp} \tag{3}$$

where k_D is the Henry's law constant, C'_H is the Langmuir capacity constant, and b is the Langmuir affinity constant. The C'_H term characterizes the amount of unrelaxed free volume in the glassy matrix, and it allows description of the nonequilibrium nature of such materials. The affinity constant, b, characterizes the tendency of a given penetrant to sorb into the excess unrelaxed volume in the nonequilibrium matrix.

Previous researchers have examined rigid polypyrrolone materials for other gas separations such as O_2/N_2 and CO_2/CH_4. Walker, Zimmerman, and Koros have studied structure−property relationships for polypyrrolone copolymers.[2,9] Permeation results are shown in Figure 1 for the O_2/N_2 separation over a variety of

† Georgia Institute of Technology.
‡ The University of Texas at Austin.
* Corresponding author: e-mail wjk@che.gatech.edu.

10.1021/ma0259261 CCC: $25.00
Published on Web 03/13/2003

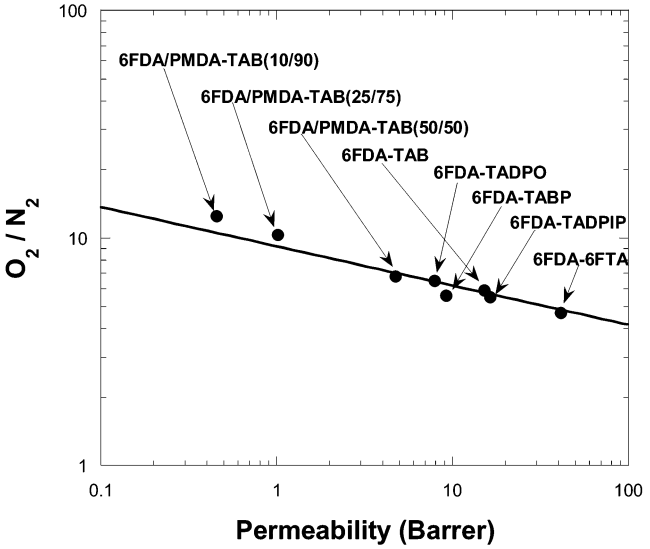

Figure 1. Previous polypyrrolone O_2/N_2 results plotted on Robeson's 1991 "upper bound" tradeoff curve.[2,9]

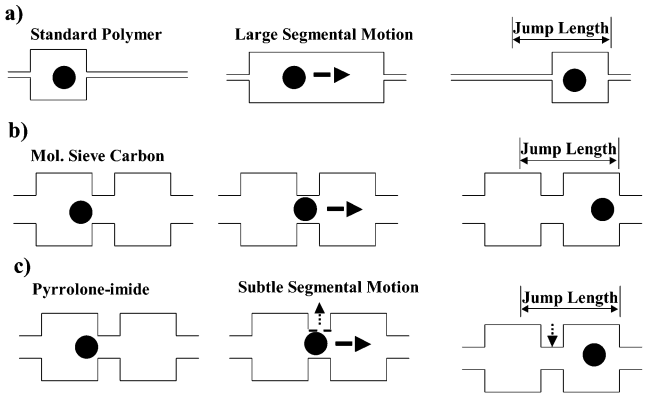

Figure 2. Idealized illustration of penetrant diffusive jumps in ultrarigid poly(pyrrolone-imide) polymers compared to conventional polymers and molecular sieving materials: (a) standard polymer; (b) molecular sieving carbon material; (c) poly(pyrrolone-imide).

polypyrrolone materials. It is clear that all of the polymers reside on or above Robeson's 1991 upper bound limit,[1] exhibiting separation properties superior to those of conventional polymeric materials, and that is why these ultrarigid polymers have been termed "pseudo molecular sieves". The reason for the high-quality separation properties of these polymers is believed to be the combination of ultra-chain rigidity and increased interchain spacing. Figure 2 illustrates an idealized picture of the poly(pyrrolone-imide) materials examined in the work here. It is believed that these materials differ from conventional polymeric materials because only subtle segmental motions are involved in the activated diffusion jump. This is more similar to molecular sieving materials, such as carbons and zeolites, where the selective pores are "frozen" within the structure. Entropic selectivity also plays a major role in the ability to discriminate between similarly sized molecules, and these effects have been discussed and demonstrated previously.[10,11] Furthermore, on the basis of the Lennard-Jones parameters (4.68 Å for C_3H_6 and 5.06 Å for C_3H_8), it is expected that molecular sieving materials able to distinguish between O_2/N_2 and CO_2/CH_4 based on diffusion considerations will also provide separation for C_3H_6/C_3H_8 based on similar size differences of the molecules. It should be noted that, while past investigations have used the kinetic diameter to represent the size of gas molecules under consideration, for higher hydrocarbons it has been found to be more practical to use the Lennard-Jones diameter as a size representation, and this concept has been discussed in more detail elsewhere.[12]

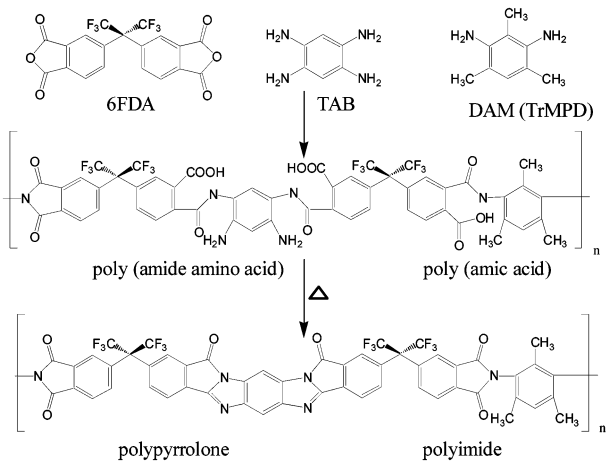

Figure 3. Synthesis of poly(pyrrolone-imide) copolymer, 6FDA-TAB/DAM.

3. Experimental Section

The monomers used in this work are shown in Figure 3. 6FDA was received from Hoechst Celanese and purified by vacuum sublimation at 220−230 °C. Trimethylphenylinediamine (DAM also known as TrMPD) was purified by vacuum sublimation at ∼85 °C. The 1,2,4,5-tetraaminobenzene tetrahydrochloride (TABH) was obtained from Aldrich in technical grade and purified via an aqueous recrystallization with activated carbon. The exact procedure is provided elsewhere.[13]

The synthesis procedure for 6FDA-TAB/DAM poly(pyrrolone-imide) copolymers is slightly modified from the synthesis of the pure polypyrrolone, 6FDA-TAB, provided elsewhere.[13] The first step of the reaction, shown in Figure 3, was conducted in DMAc solution under an inert purge with continuous stirring of the reactor. The polymer precursor was precipitated into chloroform and broken up in a blender. The polymer was filtered through a glass-fritted funnel and washed several times with chloroform. The resulting polymer was dried under vacuum at no more than 50 °C for 2 days.

Films of the precursor poly(pyrrolone-imide) copolymer were cast in a conventional manner. The appropriate amount of polymer was dissolved in dry DMAc to form a 1−2 wt % solution. This solution was stirred for at least 20 min before filtering the solution with a 0.2 μm Teflon syringe filter or alternatively filter paper from Fisher Scientific of medium porosity. The filtered solution was dispensed on a clean, level Teflon dish set on a hot plate with a surface temperature of 80 °C. The dish was quickly covered with a casting funnel to control the rate of solvent removal. Film formation generally occurred in under 8 h, and the films were then removed and placed in the vacuum oven at 100 °C for at least 12 h to ensure complete solvent removal. The second step of the reaction is then conducted (Figure 3). The films were slowly heated to 300 °C under vacuum over a period of 10−12 h. The membranes were maintained at 300 °C for 24 h and then slowly cooled to room temperature over a period of 12−24 h.

For all permeation experiments the constant volume method was employed, which utilizes a high-pressure upstream with a vacuum downstream, and this method has been described previously.[14] The downstream rise in pressure is monitored over the fixed downstream volume to determine the overall gas throughput. Film thickness measurements were made using a micrometer. The permeation area of the films was determined using Scion Image software. Gases measured

included O_2, N_2, CO_2, CH_4, C_3H_6, and C_3H_8. Ultrahigh-purity (99.99%) O_2, N_2, and CO_2 were used, and CP grade CH_4, C_3H_6, and C_3H_8 were used. Gas sorption measurements were conducted on polymeric materials using a dual-volume sorption apparatus previously described in detail[15] and similar to those described previously in the literature.[16]

The density of the polymers was measured by means of a Techne density gradient column, model DC-1. The column was prepared with calcium nitrate solution. Polymer samples were submerged and allowed to equilibrate for 24−48 h. All measurements were made at 30 °C.

Wide-angle X-ray diffraction measurements were conducted using a Phillips PW 1710 diffractometer with Cu Kα radiation of wavelength 1.54 Å. The average intersegmental distance between polymer chains or "*d* spacing" is determined through Bragg's law:

$$n\lambda = 2d \sin \theta \qquad (4)$$

where n is the order of reflection, λ is the X-ray wavelength, and θ is the angle of incidence. Amorphous materials such as polymers examined here show broad peaks due to a lack of long-range order. This technique has been demonstrated previously for polyimide and polypyrrolone materials.[2,17]

Glass transition temperatures were measured using dynamic scanning calorimetry with a Perkin-Elmer DSC 7. Glass transition temperatures were determined using the onset method. Heating runs were typically done at 20 °C/min up to 560 °C.

4. Results

Physical Properties of Poly(pyrrolone-imides). The strategy and motivation for using polypyrrolones and poly(pyrrolone-imide) copolymers lies in the fact that these ultrarigid materials can mimic molecular sieves.[9,18] In addition to rigidity, it is necessary to attempt to alternate "open" regions and "bottleneck" selective regions by tuning the polymeric matrix through the use of different monomer stoichiometry. The copolymer chosen was 6FDA-TAB/DAM, and in this case the matrix properties can be carefully adjusted by varying the tetraamine-to-diamine ratio. Figure 4 shows the structure of the 6FDA-TAB/DAM copolymer as well as 3-dimensional drawings created by HyperChem software. The first noticeable element of the 3-dimensional structures is that the 6FDA monomer (because of the CF_3 groups) must "fold" upon itself, creating disruptions along the polymer chain. Clearly, this monomer creates packing disruptions and adds to the free volume throughout the matrix. As observed in the lower drawing in Figure 4, the tetraamine monomer is planar and very flat and therefore able to pack closely to other polymer chains. Additionally, the tetraamine provides a ladder structure and hence rigidity to the material. Conversely, the methyl groups of the diamine (DAM) provide spacers within the matrix. It is also hypothesized that since the lowest energy conformation of the diamine monomer is perpendicular to the dianhydride counterpart (determined by Hyperchem software), this steric hindrance provides an additional mode in order to create space between the polymer chains. Because of the stoichiometry in the polymerization reaction, it is necessary to have alternating dianhydrides and amines. Therefore, it is a reasonable choice to allow 6FDA to comprise the dianhydride monomer and to vary the ratio of the TAB and DAM within the stoichiometry because these monomers function differently in terms of their effect on transport properties. The remainder of this paper will examine structure−property relationships varying the TAB/DAM ratio within the copolymer.

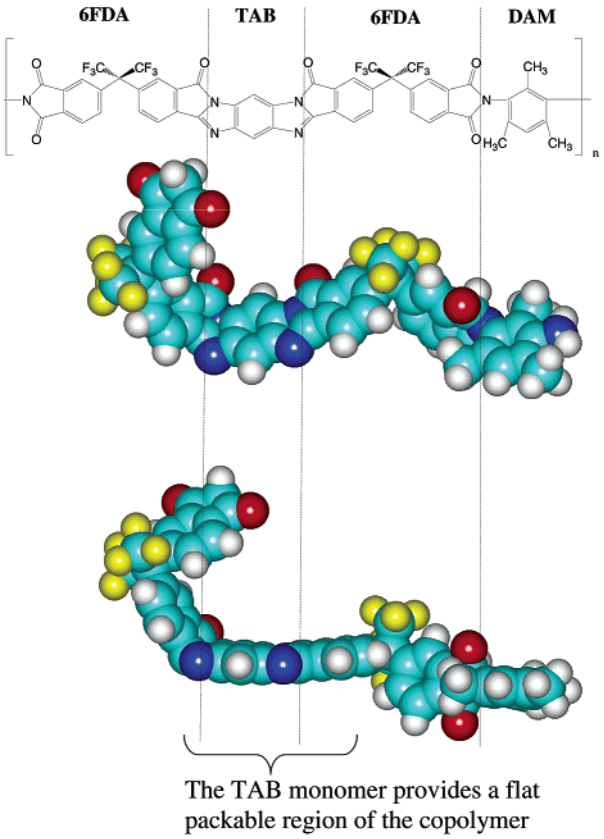

Figure 4. One unit of the 6FDA-TAB/DAM(50/50) copolymer depicted using HyperChem software.

Table 1. Physical Properties of 6FDA-TAB/DAM Copolymers

polymer	density (g/cm^3)	T_g (°C)	*d*-spacing (Å)
6FDA-DAM	1.352	375	3.7, 6.2
6FDA-TAB/DAM(30/70)	1.433	>560	
6FDA-TAB/DAM(50/50)	1.449	>560	4.2, 5.6
6FDA-TAB/DAM(75/25)	1.456	>560	4.1, 5.7
6FDA-TAB	1.486	>560	3.5, 5.7[a]

[a] Data reported previously.[2]

The density of each copolymer is shown in Table 1. There is a considerable density difference between 6FDA-DAM and 6FDA-TAB, and this is one reason these particular polymers were chosen to make up this copolymer family. Altering the TAB/DAM ratio provides a considerable amount of tunability with respect to the density of the copolymer. The T_g of the copolymers is also indicated in Table 1. The limit of the DSC was 560 °C, and it can be seen that all copolymers containing the pyrrolone segments did not show a T_g below 560 °C.

X-ray diffraction data are shown in Figure 5, and *d* spacings are provided in Table 1. In many cases two peaks are observed in the spectra, as noted previously for these types of materials.[2] From the 50/50 TAB/DAM copolymer to the 100/0 TAB/DAM copolymer the smallest spacing is reduced significantly from 4.5 to 3.5 Å; however, the larger *d* spacings remain very similar. The observation of two *d* spacings also indicates the likelihood of a bimodal distribution of free volume. Other researchers have also noted bimodal free volume distributions of glassy polymers characterized using positron annihilation lifetime spectroscopy (PALS).[19,20]

Permeation Results. It should be noted that the O_2/N_2 and CO_2/CH_4 results are presented relative to

Table 2. Permeability Coefficients and Permselectivities for Poly(pyrrolone-imide) Copolymers at 35 °C and 2 atm

polymer	P_{O_2}[a]	P_{CO_2}[a]	$P_{C_3H_6}$[a]	P_{O_2}/P_{N_2}	P_{CO_2}/P_{CH_4}	$P_{C_3H_6}/P_{C_3H_8}$
6FDA-TAB	15.2[b]	54[b]	0.09	5.9[b]	60[b]	2.6
6FDA-TAB/DAM (75/25)	15.9	73.7	0.38	5.2	44	8.0
6FDA-TAB/DAM (50/50)	30.3	155	2.3	4.6	34	23
6FDA-DAM	109	370	28.7	3.7	21	10.1

[a] Barrer = 10^{-10} cm^3 (STP) cm/(cm^2 s cmHg). [b] Data reported previously.[2]

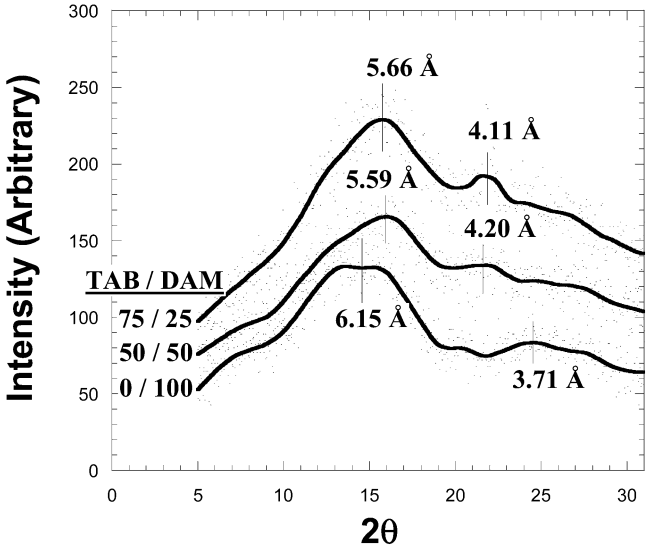

Figure 5. Wide-angle X-ray diffraction results for 6FDA-TAB/DAM copolymers.

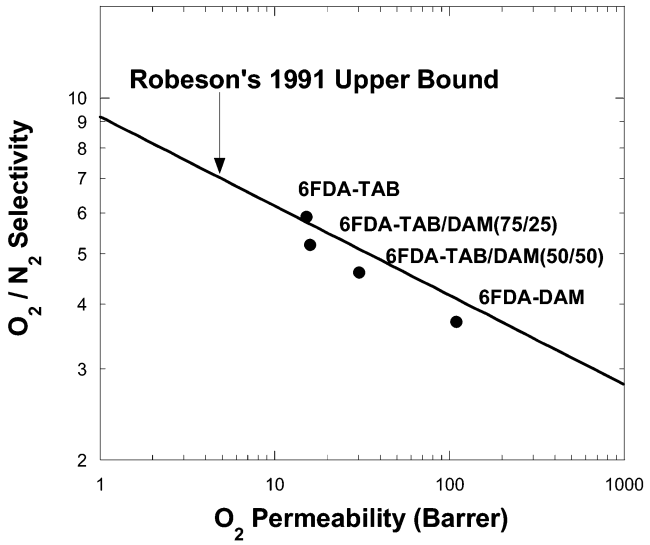

Figure 6. O_2/N_2 transport properties of 6FDA-TAB/DAM copolymers at 35 °C.

Robeson's 1991 upper bound tradeoff. Presumably, a new upper bound could be drawn today incorporating additional data over the past 12 years; however, the 1991 limit still provides an excellent representation of the state-of-the-art for these separations. Pure gas permeation results for the penetrants O_2/N_2, CO_2/CH_4, and C_3H_6/C_3H_8 are provided in Table 2. These results are also shown in Figures 6−8 plotted on the upper bound graphs for each particular separation. For O_2/N_2 separation the copolymers tested lie on or slightly below the 1991 upper bound limit, shown in Figure 6. For CO_2/CH_4, the permeation results lie on or above the 1991 upper bound limit, shown in Figure 7. The pure polypyrrolone, 6FDA-TAB, exhibits the best exchange of CO_2 permeability and CO_2/CH_4 selectivity, and this result has been published previously.[2] It is believed the ultrarigid structure of these copolymers allows them to behave as pseudo molecular sieves, and this is the reason for the high-quality separation properties. The trend in the results is very similar for both the O_2/N_2 and the CO_2/CH_4 case. Upon increasing the TAB/DAM ratio in the copolymer, the polymer becomes more rigid, more tightly packed, and the fractional free volume decreases. As expected, this results in a reduction in permeability and an increase in permselectivity with increasing TAB/DAM ratio.

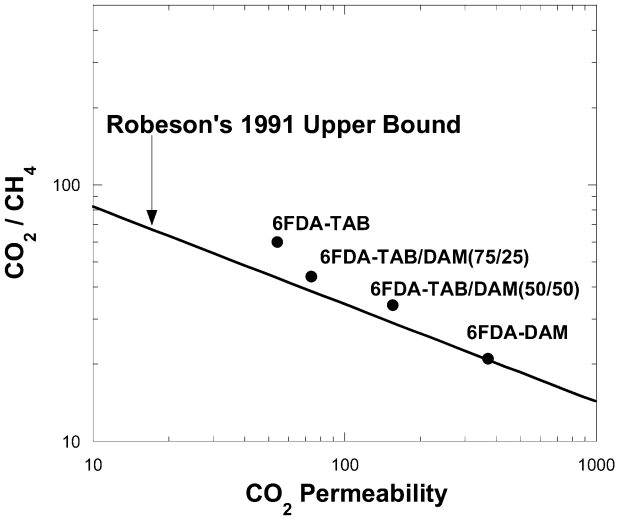

Figure 7. CO_2/CH_4 transport properties of 6FDA-TAB/DAM copolymers at 35 °C.

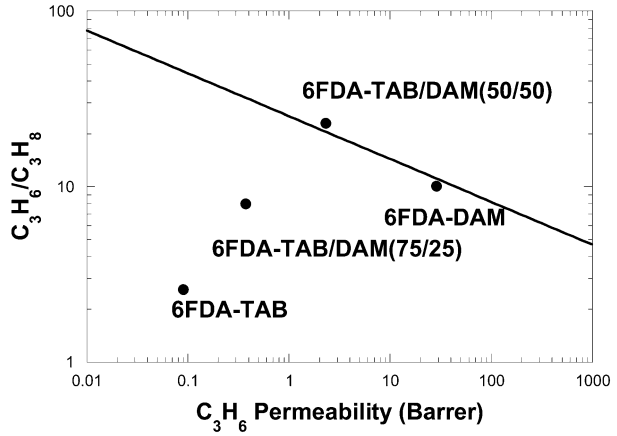

Figure 8. C_3H_6/C_3H_8 transport properties of 6FDA-TAB/DAM copolymers at 35 °C.

The C_3H_6/C_3H_8 upper bound was defined in a recent publication by the authors, which also discusses the state-of-the-art in C_3H_6/C_3H_8 separations with polymer membranes.[21] For the poly(pyrrolone-imide) materials, the C_3H_6/C_3H_8 case is quite different than for O_2/N_2 and CO_2/CH_4. In this case (Figure 8), the copolymers 6FDA-DAM and 6FDA-TAB/DAM(50/50) lie on or near the

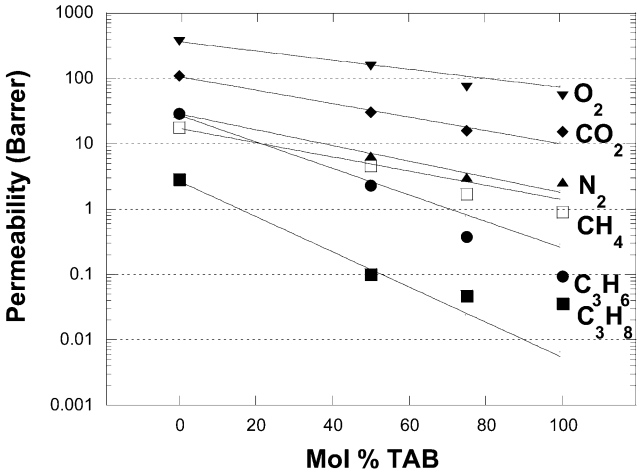

Figure 9. Gas permeability as a function of TAB/DAM ratio in the copolymer. The solid line is determined from eq 5.

upper bound trade off curve. Surprisingly, with a further increase in TAB/DAM ratio a reduction in both permeability and selectivity is observed. The resulting low C_3H_6 flux and low C_3H_6/C_3H_8 selectivity for both 6FDA-TAB and 6FDA-TAB/DAM(75/25) would be commercially undesirable under the operating conditions tested, which is surprising considering the high performance of these materials for O_2/N_2 and CO_2/CH_4 separation. For the C_3H_6/C_3H_8 case there is a selectivity maximum observed as a function of TAB/DAM ratio. For the cases considered here the TAB/DAM(50/50) copolymer lies at the height of the maximum; however, it is not known whether a copolymer lying to the right of this copolymer with a slightly lower TAB/DAM ratio might have a higher C_3H_6/C_3H_8 selectivity.

It has been proposed previously that the permeability of a copolymer can be predicted from the permeability of the pure homopolymers by the following equation:[22]

$$\ln P = \phi_1 \ln P_1 + \phi_2 \ln P_2 \qquad (5)$$

where ϕ is the volume fraction, and the subscripts 1 and 2 refer to the homopolymers, 6FDA-DAM and 6FDA-TAB in this case. In Figure 9 the permeability results for six gas penetrants are plotted on a log scale vs mol % TAB in the copolymer. The permeability measurements for 6FDA-DAM and 6FDA-TAB/DAM(50/50) were used along with eq 5 to predict the permeability results for the pure polypyrrolone, 6FDA-TAB, and the copolymer 6FDA-TAB/DAM(75/25). While it is somewhat unconventional to use permeability data from the copolymer to predict behavior of the homopolymer, we feel this is the best way to illustrate deviations from eq 5 because it is the two polymers, 6FDA-TAB and 6FDA-TAB/DAM(75/25), which are "behaving" unexpectedly (clearly shown in Figure 8). The prediction using eq 5 is represented by the solid line for each gas penetrant shown in Figure 9. Clearly for the smaller gas penetrants (O_2, N_2, CO_2, CH_4) the prediction matches the data nicely. However, for C_3H_6 and C_3H_8, deviations from the experimental data are observed. Propane permeability, in particular, is an order of magnitude larger than the predicted value for 6FDA-TAB. This illustrates that eq 5 may not always be strictly obeyed, and although it fits nicely for certain systems, it is not able to describe the trends shown here with somewhat larger molecules. This deviation from eq 5 also demonstrates in a slightly different format why the selectivity maximum is observed.

It should also be noted that within the literature for carbon molecular sieve membrane materials this surprising trend of a maximum in selectivity as a function of material structure has also been observed for a variety of gas pairs. Although the mechanism for tuning the material structure is different for the carbon materials (e.g., pyrolysis conditions) compared to the copolymers described here, the concept of adjusting the material structure to affect transport properties is very analogous. Steel has observed this surprising maximum in selectivity for C_3H_6/C_3H_8 separation as a function of pyrolysis temperature, and similarly for the poly(pyrrolone-imide) case outlined here, O_2/N_2 and CO_2/CH_4 show the expected trend of a decrease in permeability with an increase in selectivity.[23] Other researchers have also observed this trend of a selectivity maximum as a function of material structure for carbon materials with a variety of other gas separations including O_2/N_2, CO_2/N_2, CO_2/CH_4, H_2/CH_4, and He/N_2.[24−29] A separate publication will discuss fundamental reasons for this observed trend in both rigid polymeric materials and carbon molecular sieve materials.

Copolymer Sorption Isotherms. Solubility measurements made for the range of copolymers are shown in Table 3. There is no significant difference between the sorption coefficients for any particular penetrant molecule over the range of the copolymers studied. This finding is consistent with what Zimmerman found for another polypyrrolone copolymer family, 6FDA/PMDA-TAB, with gas molecules including He, O_2, N_2, CO_2, and CH_4.[13] Since these materials contain a large amount of unrelaxed free volume, there is not a considerable distinction in the overall sorption level over the range of copolymers, and this will be evaluated more extensively in the next section.

Figure 10 depicts the natural log of the sorption coefficient plotted against the Lennard-Jones energy parameter of each penetrant (which is a measure of the condensability of the molecule) for the polypyrrolone, 6FDA-TAB. There is a linear correlation, which is also consistent with previously reported trends for 6FDA-DAM.[12]

Dual Mode Analysis. The dual mode model has been able to describe sorption into glassy polymers using the assumption that two regimes are acting in tandem to enable penetrant sorption. One regime is the unrelaxed free volume of the glassy polymer, and sorption into these sites can be described by the Langmuir model. At higher pressures this free volume becomes saturated, and the Henry's law region dominates. In this case

Table 3. Sorption Coefficients and Solubility Selectivities of 6FDA-TAB/DAM Copolymers at 35 °C and 2 atm

polymer	S_{O_2}[a]	S_{CO_2}[a]	$S_{C_3H_6}$[a]	S_{O_2}/S_{N_2}	S_{CO_2}/S_{CH_4}	$S_{C_3H_6}/S_{C_3H_8}$
6FDA-TAB	0.109[b]	0.456[b]	0.982	1.49[b]	2.90[b]	1.23
6FDA-TAB/DAM (75/25)	0.063		0.820	1.54		1.03
6FDA-TAB/DAM (50/50)	0.075	0.600	0.863	1.29	2.50	1.11
6FDA-DAM	0.086	0.413	1.152	1.23	2.99	1.26

[a] S = cm^3 (STP)/(cm^3 polymer − psia). [b] Data reported previously.[2]

Table 4. Dual Mode Parameters for C_3H_6 in Various 6FDA-TAB/DAM Copolymers at 35 °C

parameter	6FDA-TAB	6FDA-TAB/DAM (75/25)	6FDA-TAB/DAM (50/50)	6FDA-DAM
k_D[a]	0.184 ± 0.012	0.191 ± 0.032	0.191 ± 0.006	0.335 ± 0.023
C'_H[b]	27.6 ± 1.04	20.1 ± 1.9	22.0 ± 0.4	25.1 ± 1.3
b[c]	0.194 ± 0.021	0.259 ± 0.080	0.263 ± 0.014	0.572 ± 0.179

[a] k_D = cm^3 (STP)/(cm^3 polymer − psia). [b] C'_H = cm^3 (STP)/(cm^3 polymer). [c] b = 1/psia.

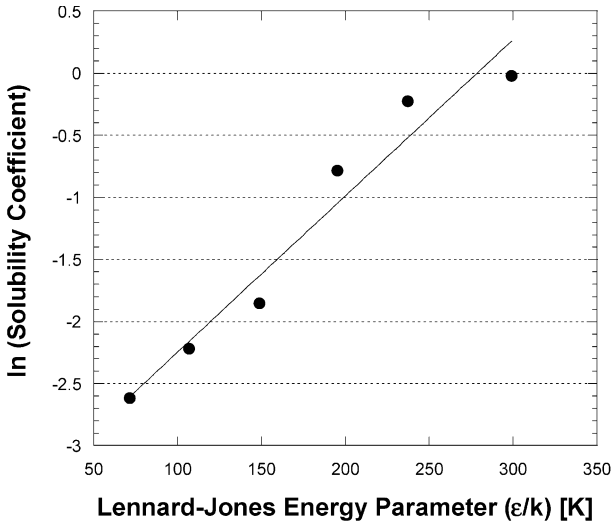

Figure 10. Log plot of solubility coefficient vs Lennard-Jones energy parameter for 6FDA-TAB.

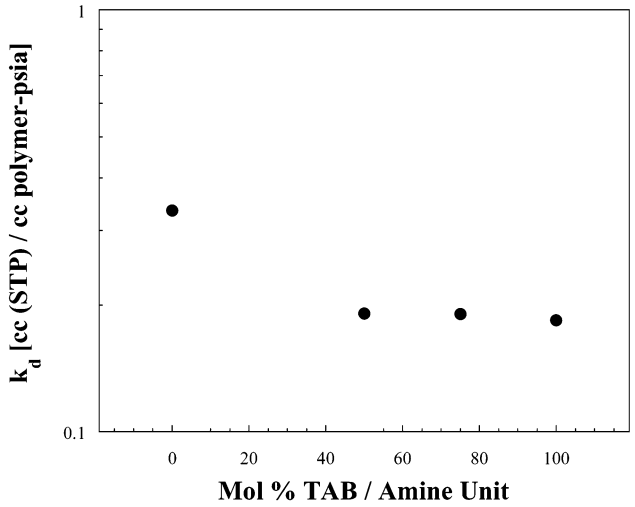

Figure 11. C_3H_6 Henry's law coefficient, k_D, as a function of the TAB/DAM ratio.

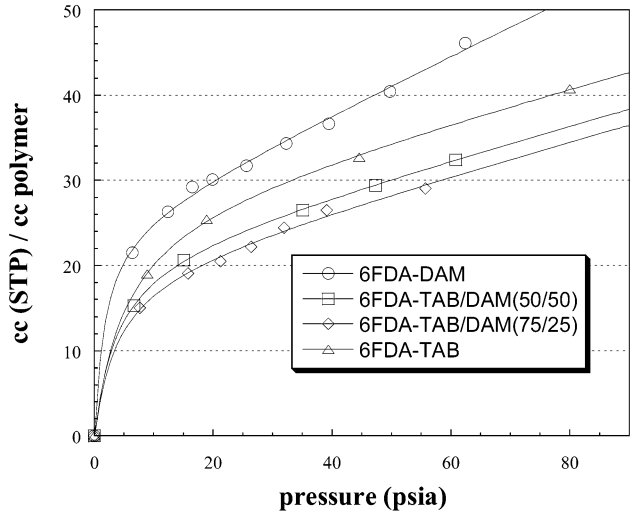

Figure 12. Sorption isotherms of C_3H_6 for the 6FDA-TAB/DAM copolymer family at 35 °C.

sorption occurs between densified polymer chains, and the sorption level is linearly proportional to the pressure or fugacity driving force. The dual mode model combines these two regimes into one model with three parameters fitted using a nonlinear least-squares regression of the sorption data. The Henry's law constant, k_D, is a measure of the penetrant's affinity for the dissolved mode of the dense polymer. Oftentimes the Henry's law constant can be correlated with the condensability of the penetrant. The Langmuir capacity constant, C'_H, measures the sorption capacity of the unrelaxed free volume. The Langmuir affinity constant, b, is a measure of the penetrant's ability to sorb into the free volume Langmuir sites.

Table 4 lists dual mode parameters of C_3H_6 for the copolymer family, 6FDA-TAB/DAM, and the sorption isotherms are shown in Figure 12. Generally speaking, there is not a strong deviation in any parameter across the range of copolymers. The Henry's law coefficient exhibits an increase with a decreasing TAB/DAM ratio (shown in Figure 11), and this is expected. As the copolymer moves toward the pure polyimide, the matrix becomes more flexible (albeit still a very rigid polymer) than the polypyrrolone. This additional chain flexibility may allow for a slight increase in C_3H_6 sorption, and thus the Henry's law coefficient is increased. It is also consistent that 6FDA-TAB is insoluble in typical organic solvents, whereas 6FDA-DAM is readily soluble. Previous studies have demonstrated that similar rigid-chain ladder polymers are insoluble in common organic solvents due to both intramolecular rigidity and intermolecular interchain attractions.[30] These interchain attractions may also *slightly* inhibit sorption in the copolymers containing pyrrolone segments. However, compared to the permeability coefficients of C_3H_6, which span greater than *2 orders of magnitude* over the range of copolymers, the increase in Henry's law coefficient is a relatively small effect. Clearly, the diffusion coefficient is the dominant factor in affecting changes in permeability, and this will be shown in the next section.

The Langmuir capacity constant, C'_H, shows no trend or extensive change over the range of copolymers (Table 4), meaning the amount of unrelaxed free volume does not appreciably change over the range of materials. Essentially, this is the reason the C_3H_6 sorption coefficients show no apparent trend.

The Langmuir affinity constant, b, shows an increasing trend with decreasing TAB/DAM ratio. It should be noted that there is more error in the fit for this parameter (5−31%), and the error could be minimized with additional data at low pressures. Again, the trends in the affinity constant are relatively small across the range of copolymers studied.

Sorption results for C_3H_8 are shown in Figure 13, and dual mode parameters are shown in Table 5. The trends for the C_3H_8 dual mode parameters generally follow

Table 5. Dual Mode Parameters for C_3H_8 in Various 6FDA-TAB/DAM Copolymers at 35 °C

parameter	6FDA-TAB	6FDA-TAB/DAM (75/25)	6FDA-TAB/DAM (50/50)	6FDA-DAM
k_D[a]	0.135 ± 0.047	0.085 ± 0.003	0.143 ± 0.012	0.184 ± 0.012
C'_H[b]	31.1 ± 5.6	23.8 ± 0.2	22.1 ± 0.7	23.7 ± 0.8
b[c]	0.056 ± 0.015	0.180 ± 0.004	0.174 ± 0.014	0.296 ± 0.030

[a] k_D = cm^3 (STP)/(cm^3 polymer − psia). [b] C'_H = cm^3 (STP)/(cm^3 polymer). [c] b = 1/psia.

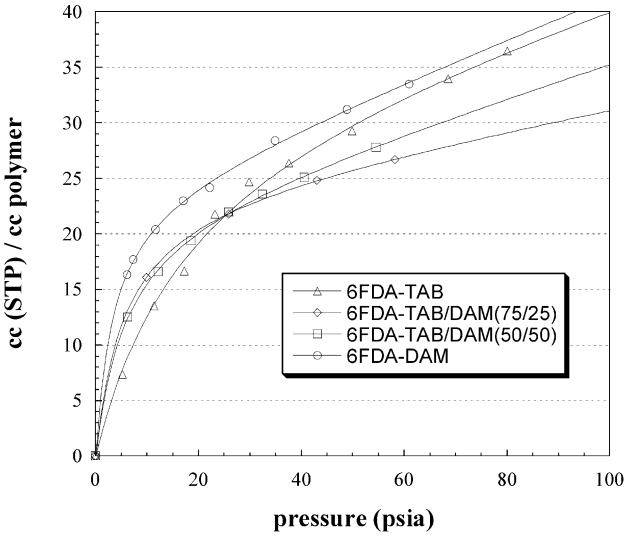

Figure 13. Sorption isotherms of C_3H_8 for the 6FDA-TAB/DAM copolymer family at 35 °C.

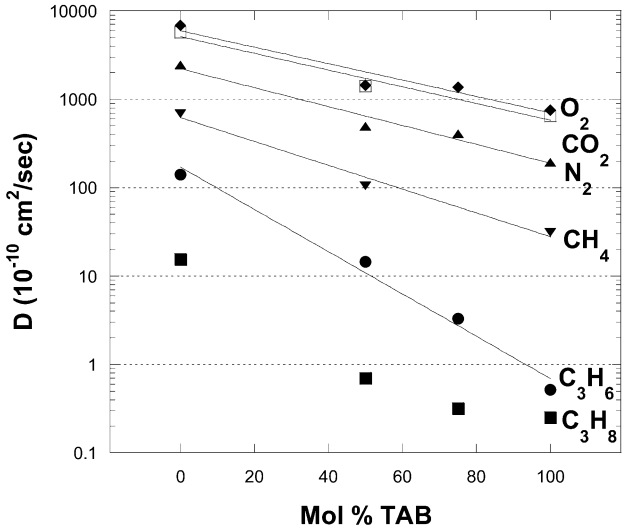

Figure 14. Diffusion coefficients of gaseous penetrants as a function of TAB/DAM ratio.

those for C_3H_6. Consistent with the C_3H_6 results, there is no observed trend in the Langmuir capacity constant. Similarly, there is an increase in the affinity constant with decreasing TAB/DAM ratio. The Henry's law constant shows a slight increasing trend. The aforementioned arguments for C_3H_6 can be applied to this case as well.

Diffusion Coefficients. Diffusion coefficients are calculated from the permeation and sorption data in Tables 2 and 3 using the solution−diffusion model. The diffusion coefficients for various gas molecules are plotted vs the TAB/DAM ratio in Figure 14. As the effective diameter of the gas molecule increases, the diffusion coefficient decreases as expected. Another noticeable trend is that, with increasing TAB/DAM ratio, the diffusion coefficient decreases in an exponential fashion. This is expected since TAB packs more efficiently than DAM. The combination of these trends leads to the observation that with increasing molecular size the diffusion coefficient experiences greater depression over the range of copolymers. This is true with the exception of C_3H_8, the largest molecule tested. The C_3H_8 curve breaks off sharply at the 6FDA-TAB/DAM(50/50) copolymer, resulting in only a moderate decrease in diffusivity from the 6FDA-TAB/DAM(50/50) copolymer to the 6FDA-TAB homopolymer. Clearly, this phenomenon leads to the permselectivity maximum demonstrated previously. Potential causes of this surprising trend will be discussed through modeling efforts in a subsequent publication. The complex effect is believed to reflect an intersection of a different characteristic penetrant size with a more or less fixed distribution of critically sized diffusive bottlenecks in the polymer. Such permanent fixed size passages exist in true molecular sieving media such as carbons (Figure 2b), and hyper rigid packing disrupted polymers (Figure 2c). In this latter type material, which are the focus of this paper, only subtle segmental motions are believed to occur. Both molecular sieve carbons and these hyper rigid polymers appear to behave differently than standard polymers (Figure 2a) in which large and less size-discriminating motions are responsible for diffusive steps.

5. Conclusions

A family of poly(pyrrolone-imide) copolymers (6FDA-TAB/DAM) was synthesized in order to investigate how the ratio of TAB/DAM monomers in the polymer chain affects transport properties of various gas molecules. For smaller molecules such as O_2/N_2 and CO_2/CH_4 a familiar trend of decreasing permeability and increasing selectivity was observed with increasing TAB/DAM ratio. Surprisingly, for C_3H_6/C_3H_8 separation a selectivity maximum was observed over the range of material structures. It was further shown that this is due to unexpected trends in the diffusion coefficient for the largest gas molecule tested, C_3H_8. This trend of a selectivity maximum over a range of material structures has also been observed for carbon molecular sieve materials for a variety of gas separations; however, this work seems to be the first indication of this trend for a family of copolymers.

Acknowledgment. The authors gratefully acknowledge bp for funding support as well as the Separations Research Program at the University of Texas at Austin. The authors also thank John Wind, Greg Pollock, Rajiv Mahajan, and De Vu for helpful discussions regarding this work.

References and Notes

(1) Robeson, L. M. *J. Membr. Sci.* **1991**, *62*, 165.
(2) Zimmerman, C. M.; Koros, W. J. *J. Polym. Sci., Polym. Phys. Ed.* **1999**, *37*, 1235.
(3) Koros, W. J.; Mahajan, R. *J. Membr. Sci.* **2001**, *181*, 141.
(4) Baker, R. W. *Ind. Eng. Chem. Res.* **2002**, *41*, 1393.

(5) Crank, J.; Park, G. S. *Diffusion in Polymers*; Academic: New York, 1968.
(6) Petropoulos, J. H. *J. Polym. Sci., Polym. Chem. Ed.* **1970**, *8*, 1797.
(7) Vieth, W. R.; Sladek, K. J. *J. Colloid Sci.* **1965**, *20*, 1014.
(8) Koros, W. J.; Chan, A. H.; Paul, D. R. *J. Membr. Sci.* **1977**, *2*, 165.
(9) Walker, D. R. B. Ph.D. Dissertation, The University of Texas at Austin, 1993.
(10) Singh-Ghosal, A.; Koros, W. J. *Ind. Eng. Chem. Res.* **1999**, *38*, 3647.
(11) Zimmerman, C. M.; Koros, W. J. *Macromolecules* **1999**, *32*, 3341.
(12) Tanaka, K.; Taguchi, A.; Hao, J. Q.; Kita, H.; Okamoto, K. *J. Membr. Sci.* **1996**, *121*, 197.
(13) Zimmerman, C. M. Ph.D. Dissertation, The University of Texas at Austin, 1998.
(14) Obrien, K. C.; Koros, W. J.; Barbari, T. A.; Sanders, E. S. *J. Membr. Sci.* **1986**, *29*, 229.
(15) Costello, L. M.; Koros, W. J. *Ind. Eng. Chem. Res.* **1996**, *31*, 2708.
(16) Koros, W. J.; Paul, D. R. *J. Polym. Sci., Polym. Phys. Ed.* **1976**, *14*, 1903.
(17) Coleman, M. R.; Koros, W. J. *J. Membr. Sci.* **1990**, *50*, 285.
(18) Zimmerman, C. M.; Koros, W. J. *Macromolecules* **1999**, *32*, 3341.
(19) Shantarovich, V. P.; Kevdina, I. B.; Yampolskii, Y. P.; Alentiev, A. Y. *Macromolecules* **2000**, *33*, 7453.
(20) Yampolskii, Y. P.; Korikov, A. P.; Shantarovich, V. P.; Nagai, K.; Freeman, B. D.; Masuda, T.; Teraguchi, M.; Kwak, G. *Macromolecules* **2001**, *34*, 1788.
(21) Burns, R. L.; Koros, W. J. *J. Membr. Sci.* **2002**, *211*, 299.
(22) Barnabeo, A. E.; Creasy, W. S.; Robeson, L. M. *J. Polym. Sci., Polym. Chem. Ed.* **1975**, *13*, 1979.
(23) Steel, K. Ph.D. Dissertation, The University of Texas at Austin, 2000.
(24) Okamoto, K.; Kawamura, S.; Yoshino, M.; Kita, H.; Hirayama, Y.; Tanihara, N.; Kusuki, Y. *Ind. Eng. Chem. Res.* **1999**, *38*, 4424.
(25) Ogawa, M.; Nakano, Y. *J. Membr. Sci.* **2000**, *173*, 123.
(26) Kusuki, Y.; Shimazaki, H.; Tanihara, N.; Nakanishi, S.; Yoshinaga, T. *J. Membr. Sci.* **1997**, *134*, 245.
(27) Kane, M. S.; Goellner, J. F.; Foley, H. C.; DiFrancesco, R.; Billinge, S. J. L.; Allard, L. F. *Chem. Mater.* **1996**, *8*, 2159.
(28) Hayashi, J.; Mizuta, H.; Yamamoto, M.; Kusakabe, K.; Morooka, S. *J. Membr. Sci.* **1997**, *124*, 243.
(29) Hayashi, J.; Yamamoto, M.; Kusakabe, K.; Morooka, S. *Ind. Eng. Chem. Res.* **1995**, *34*, 4364.
(30) Jenekhe, S. A.; Johnson, P. O. *Macromolecules* **1990**, *23*, 4419.

MA0259261